


Research Article

Remote Adipose Tissue-Derived Stromal Cells of Patients with Lung Adenocarcinoma Generate a Similar Malignant Microenvironment of the Lung Stromal Counterpart

Elena De Falco ^{1,2}, Antonella Bordin,¹ Cecilia Menna,³ Xhulio Dhori,¹ Vittorio Picchio,¹ Claudia Cozzolino,¹ Elisabetta De Marinis,¹ Erica Floris,¹ Noemi Maria Giorgiano,¹ Paolo Rosa,¹ Erino Angelo Rendina,³ Mohsen Ibrahim,³ and Antonella Calogero¹

¹Department of Medical-Surgical Science and Biotechnologies, Faculty of Pharmacy and Medicine, University of Rome "Sapienza", C.so della Repubblica 79 04100, Latina, Italy

²Mediterranea Cardiocentro, Napoli, Italy

³Department of Thoracic Surgery, University "Sapienza", S. Andrea Hospital, via di Grottarossa 1035, 00189 Rome, Italy

Correspondence should be addressed to Elena De Falco; elena.defalco@uniroma1.it

Received 19 May 2022; Revised 25 November 2022; Accepted 25 December 2022; Published 24 January 2023

Academic Editor: Dali Zheng

Copyright © 2023 Elena De Falco et al. This is an open access article distributed under the Creative Commons Attribution License, which permits unrestricted use, distribution, and reproduction in any medium, provided the original work is properly cited.

Cancer alters both local and distant tissue by influencing the microenvironment. In this regard, the interplay with the stromal fraction is considered critical as this latter can either foster or hamper the progression of the disease. Accordingly, the modality by which tumors may alter distant niches of stromal cells is still unclear, especially at early stages. In this short report, we attempt to better understand the biology of this cross-talk. In our "autologous stromal experimental setting," we found that remote adipose tissue-derived mesenchymal stem cells (mediastinal AMSC) obtained from patients with lung adenocarcinoma sustain proliferation and clonogenic ability of A549 and human primary lung adenocarcinoma cells similarly to the autologous stromal lung counterpart (LMSC). This effect is not observed in lung benign diseases such as the hamartochondroma. This finding was validated by conditioning benign AMSC with supernatants from LAC for up to 21 days. The new reconditioned media of the stromal fraction so obtained, was able to increase cell proliferation of A549 cells at 14 and 21 days similar to that derived from AMSC of patients with lung adenocarcinoma. The secretome generated by remote AMSC revealed overlapping to the corresponding malignant microenvironment of the autologous local LMSC. Among the plethora of 80 soluble factors analyzed by arrays, a small pool of 5 upregulated molecules including IL1- β , IL-3, MCP-1, TNF- α , and EGF, was commonly shared by both malignant-like autologous A- and L-MSc derived microenvironments vs those benign. The bioinformatics analysis revealed that these proteins were strictly and functionally interconnected to lung fibrosis and proinflammation and that miR-126, 101, 486, and let-7-g were their main targets. Accordingly, we found that in lung cancer tissues and blood samples from the same set of patients here employed, miR-126 and miR-486 displayed the highest expression levels in tissue and blood, respectively. When the miR-126-3p was silenced in A549 treated with AMSC-derived conditioned media from patients with lung adenocarcinoma, cell proliferation decreased compared to control media.

1. Introduction

Mesenchymal stem cells (MSC) have been described as adult multipotent stem cells, showing many relevant properties, spanning from the ability to immunomodulate and migrate to specific sites of injury to the transdifferentiation into multiple cell types [1, 2]. MSC have been considered ideal

candidates for many clinical and cell therapy applications, almost concluding that their wide applicability was also possible in cancer treatment [3].

The biological interaction between MSC and tumors is complex and enormously debated. Several controversies exist about the potential of MSC to enhance or to even arrest tumorigenicity, not only of their double-faced behavior such

as tumor-tropism (hence tested as vehicles for anticancer genes targeting cancer cells or as enhancement of the CAR-T immunotherapy) [4, 5] and immunomodulatory features but also prometastatic functions [6–8], transdifferentiation into cancer-associated fibroblasts and drug resistance [9], the parallel ability to overturn the immune system [10–13], and activation of autophagy and neo-angiogenesis [14], therefore contributing to tumor evolution. This discrepancy also includes exosome-derived MSC, considered both an intriguing therapeutic tool for drug delivery and the main biological mediators of several supporting tumor molecular processes [15]. Moreover, from a clinical standpoint, it has been recognized that the endogenous recruitment of MSC (of different origins including adipose) from systemic niches may occur by tumor secretion of inflammatory soluble factors [16] and that a correlation exists between circulating mesenchymal tumor cells and stage of tumor development [17, 18].

This scenario is also complicated by recent indications about the heterogeneity of MSC and the phenotypic and functional changes potentially caused by tumors. For instance, adipose tissue and bone marrow-derived MSC have shown differences with respect to stem cell content and epigenetic states [19, 20]. Besides, MSC obtained from diverse sources such as heart, dermis, bone marrow, and adipose tissue have been reported as genotypically different, expressing different levels of embryonic stem cell markers such as OCT-4, NANOG, and SOX-2 [21], and biological properties including angiogenesis and secretome [20]. When MSC are derived from cancer tissues, they show altered molecular and functional properties [22–24], suggesting that the tumor characteristics such as benignity or malignancy could influence the environment where MSC is located.

From a biological standpoint, the evolution from a local to a systemic cancer microenvironment can be driven either by phenotypically altered cancer-associated cells (fibroblasts and endothelial cells), which organize clusters of systemic spreading cells or by niche-to-niche recruiting phenomena from the bone marrow to the tumor site [25, 26]. However, the thorny question is still centered on the modality by which cancer can control the systemic environment, influencing remote “normal” and nonbone marrow stem cell-derived niches including distant MSC niches, particularly at the early stages of the tumor, which are of paramount biological and clinical relevance to understand cancer progression.

Assuming that the pathophysiology of cancer can be interpreted as a systemic disease, in this short report we attempt to investigate whether MSC-derived microenvironments at a remote site from a tumor can be already altered at the early stages of lung adenocarcinoma [27].

2. Methods

2.1. Surgical Specimen Collection and Clinical Database. At the end of the surgical procedure, a small sample of mediastinal adipose [1, 2] and lung tissue was collected by electrocoagulation from patients undergoing surgical procedures for hamartochondroma and non-small cell lung

carcinoma (NSCLC). Surgical procedures were conducted at S. Andrea Hospital, Rome. Written informed consent was obtained from patients, before starting all the surgical and laboratory procedures. Patients with NSCLC and staging T1N0M0 G1 were selected, whereas subjects with metastasis have been excluded from the study.

2.2. Isolation and Characterization of AMSC and LMSC. AMSCs were isolated and characterized as previously described [1, 2, 28]. Patient’s characteristics are described in supplementary Tables 1a and 1b. Lung specimens were chopped with a scalpel and scissors in a 100 mm Petri dish, then gently transferred into a clean 100 mm Petri dish to allow tissue adherence. A complete growth medium composed of DMEM high glucose (Invitrogen) supplied by 10% FBS, antibiotics, and L-glutamine (all Gibco) was added to the fragments. Plates were incubated at 37°C in a fully humidified atmosphere of 5% CO₂, avoiding shaking the plates at least for 72 hours. Half of the medium was replaced with a fresh complete medium every three days.

2.3. Isolation of Lung Adenocarcinoma Cells and In Vitro Conditioning with MSC-Derived Supernatants. Human primary lung adenocarcinoma cells (LAC) were isolated as we already previously described [29]. The cells obtained were cultured in a complete medium (DMEM-F12, penicillin-streptomycin, L-glutamine, nonessential amino acids, sodium pyruvate, all Gibco, Monza, Italy, and 5% FBS, Lonza, Milan, Italy). Lung adenocarcinoma A549 was purchased by ATCC and cultured in DMEM-F12 supplemented with 10% FBS (All Gibco). AMSC and LMSC supernatants derived from patients with hamartochondroma or NSCLC were collected between passages 3–6, then stored at –80°C until use.

A549 or human primary LAC was conditioned by removing their own medium and replacing it with A- or LMSC-derived conditioned media diluted 1:1 with basal media of A549 or LAC. Every 3 days, 1/5 of the whole medium was discarded and fresh media was replaced. Cells were cultured according to the time course indicated in the study.

2.4. Proliferation, Clonogenic Assay, and FACS Analysis. Both LAC and A549 were seeded onto 96-well plates (150 cells/well) and incubated for 24 hours with DMEM low glucose 10% FBS [29]. Then cells were exposed to the different conditioned media collected from AMSC and LMSC for up to 7 days. Cells treated with the basal medium were used as a control. The effect of conditioned media on cell viability was evaluated by the MTS assay. Briefly at 3, 5, and 7 days after treatment, 20 µl of MTS reagent were added to each microculture well, and plates were incubated for 2 hours at 37°C, after which absorbance at 492 nm (optical density) was measured using a microplate reader.

To test the secondary colony forming efficiency (CFU) assay, LAC or A549 were seeded at passage 3 at low density (10 cells/cm²) [29] in AMSC- and LMSC-derived

conditioned media for 14 days and incubated at 37°C. Colonies produced were fixed with 4% paraformaldehyde and then stained with Giemsa (Sigma, Milan, Italy) for 1 h and counted by optical microscope. A cluster with >50 cells was considered a colony [20].

FACS analysis was performed to investigate the percentage of apoptotic cells after stimulation with AMSC-derived conditioned media as previously reported [30, 31]. Briefly, semiconfluent cultures were harvested with Accutase (Sigma-Aldrich) and stained for 30 minutes with 5 μ l AnnexinV-FITC antibody (Invitrogen Cat. number 88-8005-74) and counterstained with propidium iodide (10 ng/mL, Invitrogen, Cat. number 88-8005-74) according to the manufacturer's protocol for adherent cells. Data acquisition was performed on a FACS-Aria II platform equipped with FACSDiva software (BD Biosciences). All flow cytometry data were analyzed with FlowJo software (FlowJo LCC, Ashland, USA).

2.5. Analysis of the Autologous A- and LMSC-Derived Secretome. The evaluation of the different microenvironments was performed on collected supernatant obtained from both A- and LMSC in patients with lung adenocarcinoma and hemartochondroma. C-Series Human Cytokine Antibody Array C5 (RayBiotech, Inc) was used for simultaneous semiquantitative detection of 80 multiple cytokines/growth factors as previously described [31]. Briefly, an equal volume of collected undiluted supernatants was incubated by gentle shaking overnight at 4°C on the membrane of the kit C-Series Human Cytokine Antibody Array C5. Chemiluminescence was employed to quantify the spots (at the same time exposure was used for all membranes) and each spot signal was analyzed by ImageJ. The samples were normalized on positive control means (six spots in each array) and then values were expressed as a percentage. To visualize the overall changes in cytokines array average data, results were graphed as log (2) in heatmap analysis by using the pheatmap R package in the RdYlBl color scale (from 0 to 7 expression levels). Cytokines with zero values in all replicates were ruled out.

2.6. Interaction and Functional Evaluation of Cytokines Network within the Microenvironments and miRNA Target Interaction Analysis. Correlation analysis between the cytokines expressed by A- or LMSC-derived benign and malignant microenvironments, was obtained by calculating the fold changes between these two conditions. A fold change threshold of >1.2 was considered as upregulated [32]. The analysis for known protein interaction was performed on commonly upregulated cytokines between A- and LMSC by using the STRING software (<https://string-db.org/>, version 11.5) [33], building the whole network according to the high confidence setting (0.7) and default options. The pathway and process enrichment analysis were performed using Metascape as already described elsewhere [34].

The miRNA-target interaction analysis was performed by using the "multiMiR" R package and reviewing literature employing lung cancer as a keyword. The list of miRNAs in

the R package was obtained using the `get_multir` function setting only on validated data and the databases queried were miRecords, miRTarBase, and TarBase.

2.7. A549 Transfection with AntagomiR-126-3-p and Digital Droplet PCR. A549 were cultured in complete media. For silencing endogenous miR-126-3p, we perform the same protocols we recently described with some modifications [34]. Briefly, A549 were transfected plating at a density of 1.5×10^4 /24 wells with DMEM-F12 10% FBS. A mix composed of 25 picomoles LNA_126 (miRCURY LNA miRNA inhibitor (5)—3'Fam, Cat. N. 339121, Qiagen) or 25 picomoles control (miRCURY LNA miRNA inhibitor control (5)-No Modification Fam, Cat N. 339126, Qiagen) in Opti-MEM reduced serum media and lipofectamine (1 μ l/100 μ l Opti-MEM, RNAiMAX, Invitrogen, Cat. N. 56531) was added to the A549 and incubated for 5 hours. After that, the medium was removed, and new DMEM-F12 10% FBS as control and supernatants of AMCSs were added to the cells for up to 24 hours of total transfection. To verify transfection, cells were subjected to digital droplet PCR, to quantify the decrease of copy numbers of the miR-126-3p.

Total RNA was extracted from the A549 cell pellet by miRNeasy kit (Qiagen, GmbH, Hilden, Germany) according to the manufacturer's recommendation. Purified RNA was quantified at a NanoDrop spectrophotometer and used for reverse transcription reaction by the TaqMan miRNA Reverse Transcription Kit and miR-126-3p-3p-specificstem-loop primers (Applied Biosystem, Carlsbad, CA, USA). 10 ng of total extracted RNA, 1 \times stem-loop RT primer specific for miRNAs, 3.33 U/ μ L MuLV reverse transcriptase, 0.25 U/ μ L RNase inhibitor, 0.25 mM dNTPs, and 1 \times reaction buffer were run in a total reaction volume of 15 μ L and incubated at 16°C for 30 min, 42°C for 30 min, and 85°C for 5 minutes in a thermal cycler. Afterward, digital droplet PCR was performed by employing the QX200 ddPCR system (Bio-Rad, Hercules, CA, USA), using TaqMan MicroRNA assay specific for hsa-miR-126-3p (Applied Biosystem) as we reported [34, 35]. The reaction mix was assembled with 1.3 μ l of miR-126-3p-specific cDNA, 1 \times TaqMan MicroRNA miR-126-3p-specific assay, and 1 \times ddPCR supermix for probes (no dUTP) (Bio-Rad) in 20 μ l of total volume. The mix was loaded into droplet generator cartridges with 70 μ l droplet generation oil for probes (Bio-Rad). Each reaction mixture was partitioned by the QX200 droplet generator machine (Bio-Rad) into approximately 20,000 droplets. Then, 40 μ l of droplets were placed into a PCR 96-well plate that was sealed using a pierceable foil heat seal and a PX1 PCR plate sealer (Bio-Rad). The PCR was performed on the T-100 thermal cycler (Bio-Rad) under the following conditions: 10 minutes at 95°C, 30 seconds at 94°C and 1 minute at 60°C for 40 cycles with a ramp speed of 2°C/s, 98°C for 10 min, and held at 4°C for at least 40 minutes. Droplets were assessed with a QX200 droplet reader machine and QuantaSoft Software (Bio-Rad). The threshold between the positive and negative droplet clusters was manually set for all samples. ddPCR data are presented as absolute copies of transcripts/ μ l of reaction sample \pm Poisson 95% confidence intervals.

2.8. MiRNA Extraction and Quantification. MicroRNA extraction was performed from paraffin tumor tissue sections (RNeasy DSP FFPE Kit, Qiagen) and the RNA amount was determined using a NanoDrop spectrophotometer. Differently, miRNAs obtained from serum patients (200 μ l) were isolated by the Qiagen miRNeasy kit with further modifications for biofluids applications. Syn-cel-miR-39 spike in synthetic RNA (Qiagen) was added to monitor extraction efficiency. Afterward, on both tissue sections and sera samples the reverse transcription was performed using the “MiRCURY LNA Reverse Transcription Kit” (QIAGEN) in ThermoMixer 5436 (Eppendorf, Italy) according to the following protocol: 42°C for 60 seconds, 95°C for 5 minutes, 4°C forever [33].

Selected miRNA levels such as hsa-miR-101, hsa-miR-126-3p, hsa-miR-486, and hsa-Let-7g were quantified by relative quantification using Qiagen LNA-based SYBR green detection method (miRCURY LNA miRNA PCR assay-Qiagen). Briefly, 3 μ l of cDNA was used on the Applied Biosystems 7900HT machine, adding the relevant ROX concentration to the qPCR mix [33]. The relative miRNA expression was calculated using hsa-miR-16 as endogenous control with the $2^{-\Delta\Delta C_t}$ method for cancer tissues and miR-16/miR-39 for sera [33].

2.9. Statistical Analysis. The results were expressed as the arithmetic mean \pm standard deviation (SD) for at least 3 repeated individual experiments for each sample group. Statistical differences between the values were determined by Student's *T*-test, with a value of $p < 0.05$ was considered statistically significant.

3. Results

Firstly, we investigated if early-stage lung adenocarcinoma could influence the biological behavior of MSC according to (1) their own tissue source (autologous lung or mediastinal adipose tissue-derived MSC isolated from a tumor-free nearby or remote area, respectively) and (2) the biological feature of the lung tumor (malignant or benign defined by the histological analysis) where the MSC was derived from. To this aim, we conditioned the A549 cell line with supernatants of autologous lung or adipose-derived MSC (LMSC or AMSC) derived in parallel from patients with benign disease (pulmonary hamartochondroma) or malignant tumor (early-stage lung adenocarcinoma, see supplementary Tables 1a and 1b). We tested both cell proliferation (at 0, 3, 5, and 7 days) and the clonogenic capacity of A549. The experimental plan is depicted in Figure 1(a). Results showed a significant increase of A549 cell proliferation at 5 and 7 days compared to control (Figure 1(a), $p < 0.001$ both vs control) after conditioning the lung tumor cell line with supernatants derived from LMSC or AMSC.

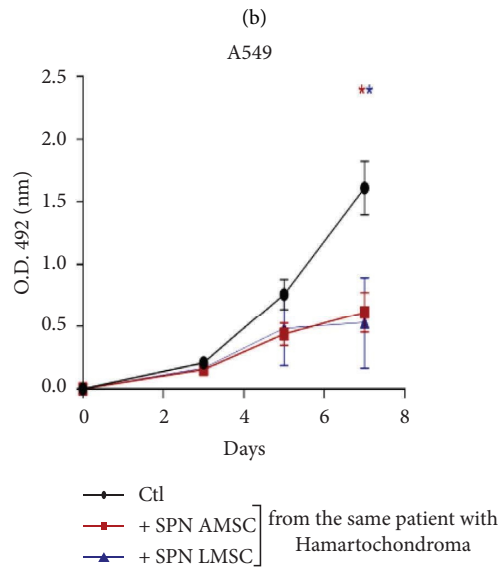
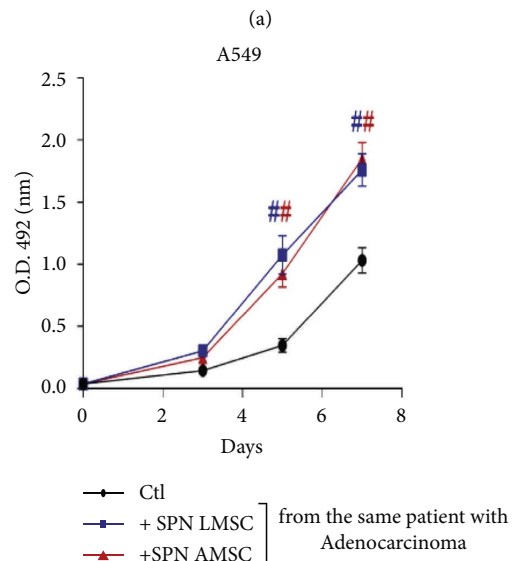
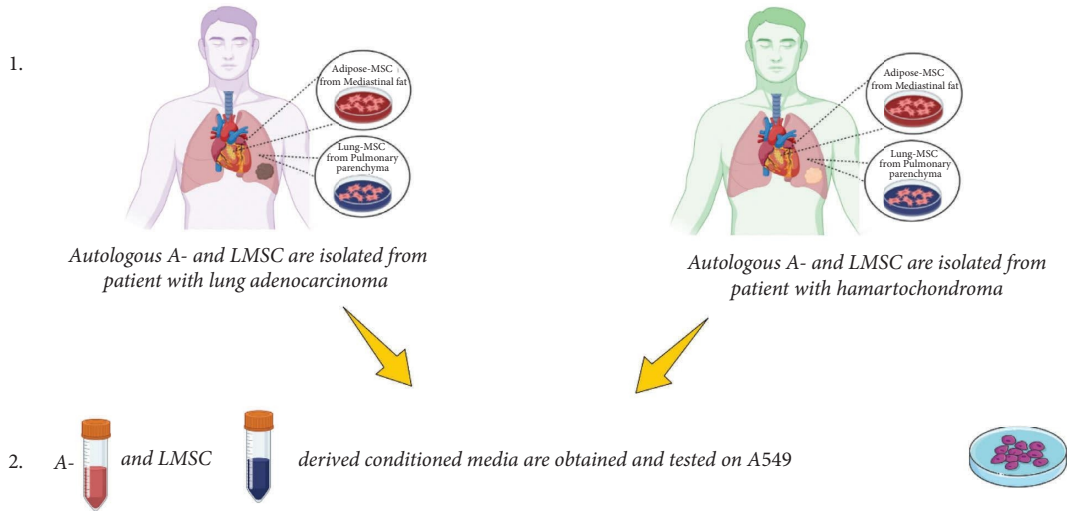
When A549 were cultured with supernatants derived from autologous LMSC or AMSC both obtained from patients with pulmonary hamartochondroma, A549 proliferation decreased compared to control (Figure 1(c), day 7 $p < 0.05$ both vs control). The stimulus with conditioned

media of benign or malignant origin did not increase apoptosis of A549 compared to control over time as demonstrated by the percentage of double-positive Annexin V/Iodide propidium cells detected by FACS analysis (Supplementary Figure 1). This result has suggested that no apoptotic effect was related to both tumor microenvironments, apart from the physiological cell turnover similar to controls.

Interestingly, a similar scenario was also reproduced regarding the clonogenic capacity of A549, where only mediastinal AMSC derived from patients with early-stage lung adenocarcinoma were able to enhance the clonogenicity respect to control (Figure 1(c), $p < 0.05$ vs control). The conditioning of A549 with supernatants derived from L- or AMSC of patients with pulmonary hamartochondroma, did not alter the clonogenic capacity of A549 (Figure 1(c)).

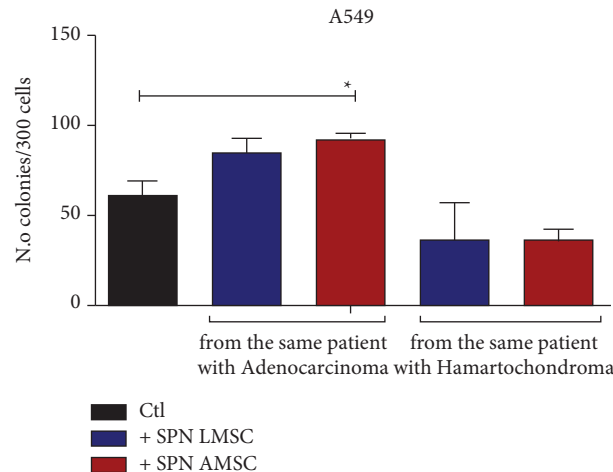
Afterward, we verified whether the same effects were also reproducible on early-stage human primary lung adenocarcinoma cells (4 lines of LAC staging T1/N0/M0 G1), by employing the same supernatants as for the A549 cell line. The experimental sequence is described in Figure 2(a). Notably, both supernatants from autologous LMSC and AMSC (because derived from the same subject) of patients with lung adenocarcinoma were able to sustain cell proliferation of LAC cells similarly to controls at all time points (Figure 2(b), $p > 0.05$). Differently, conditioned media of autologous L- or AMSC obtained from patients with pulmonary hamartochondroma, were able to decrease cell proliferation of LAC compared to controls at days 5 and 7 (Figure 2(c), day 5 LMSC $p < 0.001$, AMSC $p < 0.05$ vs controls; day 7 both LMSC and AMDC $p < 0.001$ vs controls). Coherently, we also found a significant enhancement of the clonogenic ability of LAC after the culturing with supernatants of autologous LMSC or AMSC derived from patients with early-stage lung adenocarcinoma (Figure 2(d), $p = 0.04$ LMSC and $p = 0.02$ AMSC vs controls). Conditioned media derived from autologous L- or AMSC of patient with hamartochondroma decreased or did not alter the clonogenic capacity of LAC cells (Figure 2(d), $p = 0.011$ LMSC vs controls).

We then evaluated if these effects entailed also a different paracrine signature of autologous MSC-derived microenvironments. Thus, we screened a panel of 80 pro- and anti-inflammatory cytokines and growth factors excreted by both sources of MSC in the conditioned media. Results analyzed through the heatmap (soluble factors with no expression in both L- and AMSC were ruled out) revealed that the secretome of both autologous L- and AMSC of patients with early-stage lung adenocarcinoma was similar (Figure 3(a)), therefore suggesting a comparable in vitro microenvironment. Interestingly, supernatants derived from AMSC of patients with hamartochondroma exhibited a more heterogeneous profile of soluble factors with respect to that derived from the corresponding autologous MSC counterpart in the lung (Figure 3(b)). Afterward, we further examined these secretomes. By keeping constant the source of the stromal fraction during the analysis, we calculated the increasing ratio of the soluble factors between malignant and benign microenvironments. An upregulation ratio of >1.2 was set as



(c)

FIGURE 1: Continued.



(d)

FIGURE 1: (a) Experimental design of the study on A549 cell line. 1 and 2 represent the steps of the experiments. (b) A549 proliferation by MTS assay by employing supernatants of autologous A- and LMSC-derived from patient with lung adenocarcinoma or (c) hamartochondroma. (d) Clonogenic assay on A549 with the corresponding autologous supernatants of B and C $N=4$ different conditioned media for each source of A- and LMSC. Samples were normalized on time 0. * $p < 0.05$; # $p < 0.001$.

a cut-off. Then, we sought for those common cytokine or growth factors upregulated among the two microenvironments and we generated a functional protein association network with the STRING software. Results showed a shared upregulation of 6 soluble factors including EGF, IL-1 β , IL-3, TNF- α , CCL2, and SPP1 (osteopontin). Notably, the STRING analysis which identifies protein-protein interaction, also displayed that all cytokines but SPP1 were strictly interconnected in the same cluster with a high confidence score of 0.7. Afterward, we used Metascape for the pathway enrichment analysis of this network, and we found that the most significant terms within the cluster consisting of EGF, IL-1 β , IL-3, TNF- α , CCL2 were associated with lung fibrosis and proinflammatory/fibrotic mediators (Figure 3(d)).

These results indicated a potential biological supporting tumor behavior of AMSC localized in remote areas even at the early stages of the disease. Thus, to validate this aspect, we attempt to similarly “educate” in vitro the benign AMSC obtained from a patient with hamartochondroma towards a biological “malignant-like” behavior, by reversing the experiment and culturing benign AMSC for 7, 14, and 21 days with the sole supernatants produced by LAC cells. Afterward, the same conditioned media produced by AMSC after conditioning with adenocarcinoma was removed and replaced on A549 cells which were tested for cell proliferation. We found a significant increase in cell proliferation of A549 at 14 and 21 days of tumor preconditioning compared to day 7 (Figure 4, $p < 0.001$ both).

Considering the analysis of the malignant and benign secretome of A- and LMSC (Figures 3(a)–3(d)) and that miRNAs have been demonstrated as an eligible candidate to mediate a long-distance paracrine effect, to instruct MSC and endothelial cells in lung cancer [36], we performed a computational analysis using the miRNA-target prediction

tools miRecords, miRTarBase, and TarBase combined to a revision of the literature on lung cancer of miRNAs targeting the pool of the 5 cytokines. We found four miRNAs including miR-126, 101, 486, and let-7-g. To validate the four miRNAs, we explore their expression levels on matched lung cancer tissues and samples of blood from the same set of patients employed to isolate LAC cells. Results showed that among all analyzed miRNAs the miR-126 displayed the highest expression in the lung cancer tissue (Figure 5(a), $p < 0.01$ and $p < 0.001$), differently from the circulation where is the miR-486 to show the highest levels (Figure 5(b), $p < 0.05$ and $p < 0.01$).

The miR-126 is described as one of the most important differentially expressed miRNAs in lung tumors [37] and a key miRNA regulating the pathogenesis [38] and angiogenesis of NSLC [39]. We also recently showed the angiogenic property exerted by miR-126 in endothelial cells [34]. Thus, to investigate the proliferative effects of only cancer cells by respective miR-126, we firstly evaluated in A549 by digital droplet PCR if the AMSC-derived conditioned media obtained from patients with lung adenocarcinoma was able to increase the levels of miR-126-3p. Results have shown that the treatment did not significantly increase the number of copies of miR-126-3p up to 7 days compared to the corresponding physiological levels (Figure 6(a)). Afterward, we knocked down the miR-126-3p in A549 (the recipient cells) by small interfering-based experiments at 24 hours (which was the best time performing, data not shown), halving the number of copies in cells (Figure 6(b)). After silencing, cells were reconditioned with the AMSC-derived supernatants from patients with lung adenocarcinoma and the MTS assay was performed. Notably, cell proliferation was significantly decreased only when miR-126-3p was silenced compared to the scramble (Figure 6(c), $p < 0.05$). This effect was not reproducible in A549 silenced for miR-126-3p but conditioned with the basal media of the cells (Figure 6(d)).

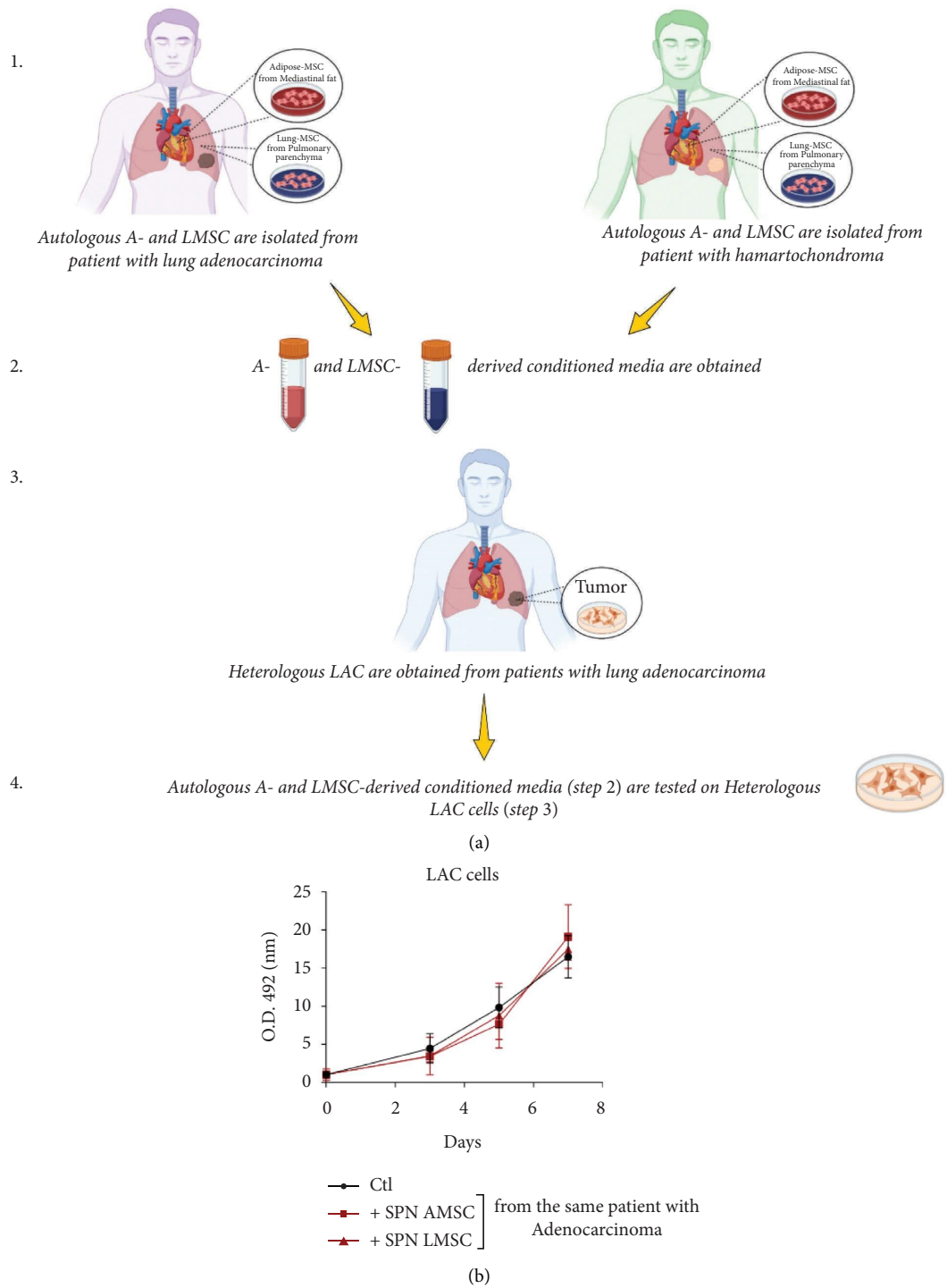


FIGURE 2: Continued.

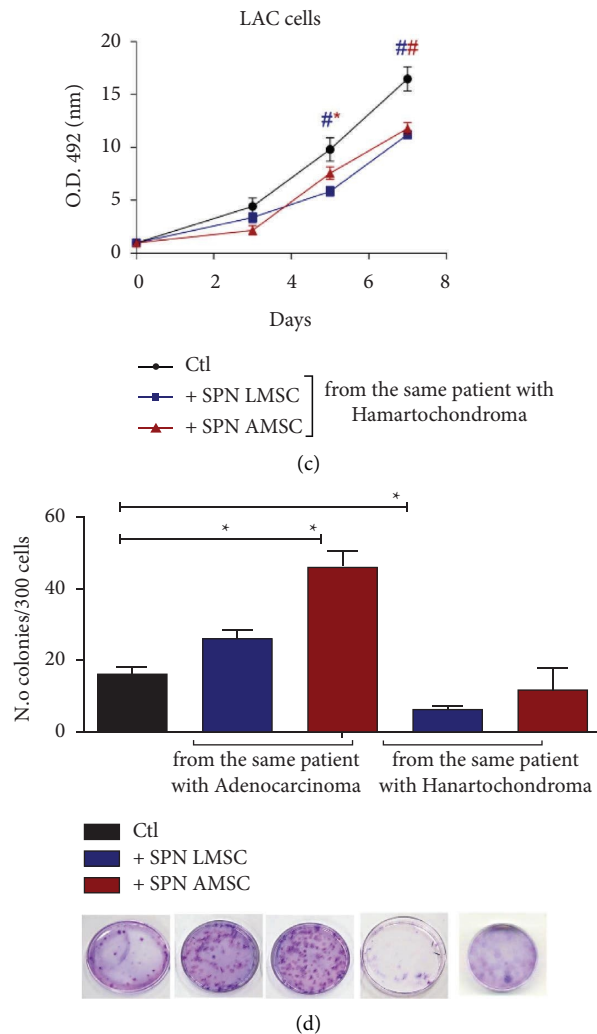


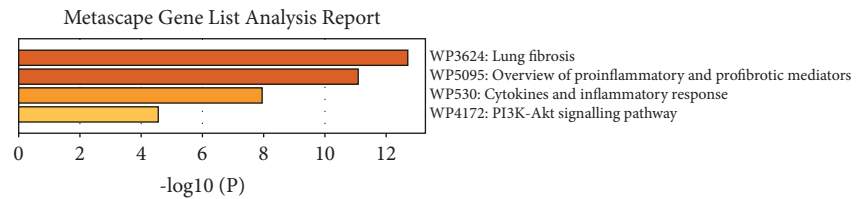
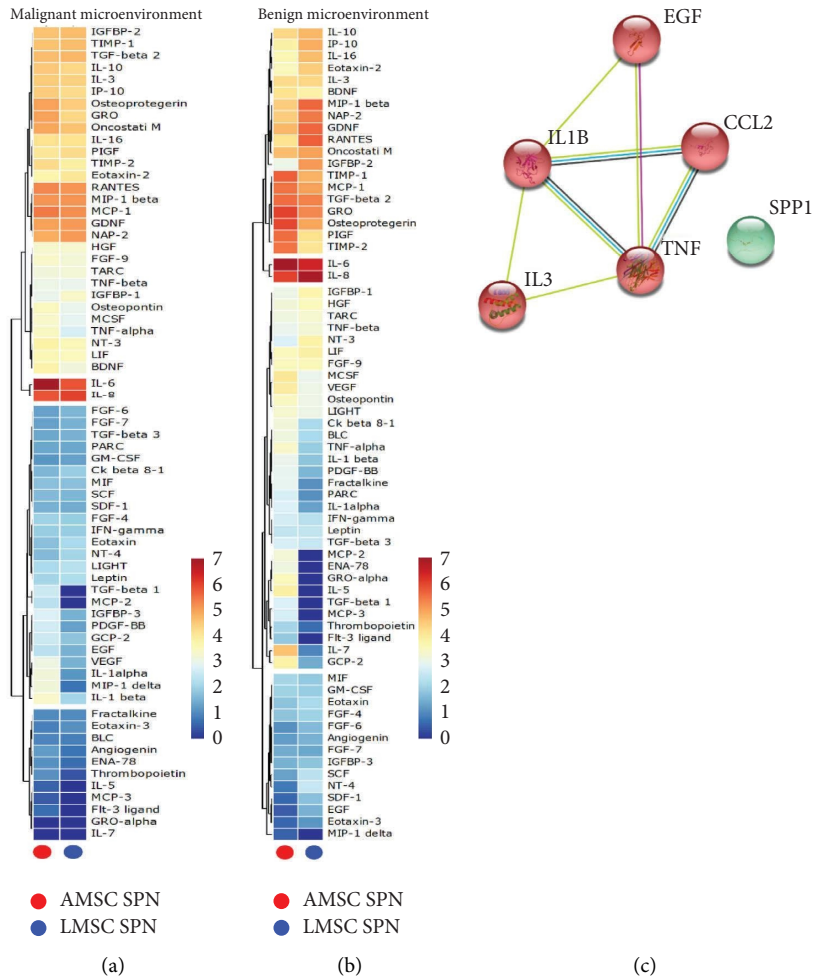
FIGURE 2: (a) Experimental design of the study on human primary lung adenocarcinoma cells (LAC). From 1 to 4 are represented the steps of the experiments (b) LAC proliferation by MTS assay with supernatants of autologous A- and LMSC-derived from patient with lung adenocarcinoma or (c) hamartochondroma. (d) Clonogenic assay of heterologous LAC with the corresponding autologous supernatants of B and C. Below the graph representative images of Giemsa staining of the clones generated by heterologous LAC cells after 3 weeks of culture in presence of autologous A- or LMSC-derived conditioned media. $N = 4$ different conditioned media for each source of A- and LMSC. * $p < 0.05$; # $p < 0.001$.

4. Discussion

This short report highlights how the tumor microenvironment is already defined at early stages, such that the stromal fraction can be influenced even at remote sites and in absence of metastasis. Intriguingly, remote AMSC derived from subjects with lung adenocarcinoma, are permissive to cell proliferation and clonogenic properties when tested on both A549 and LAC cells similar to the stromal lung counterpart. Oppositely, this effect is lost in “benign conditions.” The first important point of novelty of our brief study is that we have been able to isolate both A- and LMSC within the same patient (autologous stromal cells), therefore ruling out the variability in biological performance within the individual. A further point of originality is that our study has been focused on the early stages of lung adenocarcinoma, which has been currently given more clinical

attention. Accordingly, we have shown that at the early stages of the tumor, malignant-like microenvironments are already generated from AMSC at remote sites, and they can be overlapped with the lung stromal counterpart, which is tumor adjacent. This is in line with the concept that cancer cannot be interpreted only as a local disease, but rather than a systemic disorder [40, 41] and with the concept of tumor permissive microenvironment as the result of the interaction between stroma and cancer [42]. Our data extend this idea also to the early stages of the tumor and not only when metastasis occurs [43]. In fact, several pieces of evidence already exist regarding cancer cell spreading, considered a very early event [44].

The biological alterations we have highlighted here, are centered on the microenvironment, which is considered a critical hallmark to elucidate mechanisms of cancer plasticity [45] and where the stromal fraction exerts a critical



GO	Category	Description	Count	%	Log10 (P)	Log10 (q)
WP3624	WikiPathways	Lung fibrosis	*5	83.33	-12.70	-8.35
WP5095	WikiPathways	Overview of proinflammatory and profibrotic mediators	*5	83.33	-11.11	-7.06
WP530	WikiPathways	Cytokines and inflammatory response	3	50.00	-7.95	-4.38
WP4172	WikiPathways	PI3K-Akt signaling pathway	3	50.00	-4.54	-2.17

*Count 5: IL-1 β , IL-3, MCP-1, TNF- α , EGF

(d)

FIGURE 3: (a) and (b) Hierarchic clustering heatmap based on the cytokine arrays of autologous A- and LMSC-derived conditioned media from patients with lung adenocarcinoma and hamartochondroma (malignant and benign microenvironments, respectively). The red-yellow and the blue range colors indicate cytokines with high and low average levels, respectively. (c) Protein-protein interaction network generated by STRING database on the 6 upregulated cytokines commonly shared by autologous A- and LMSC when their malignant and benign microenvironments are compared. The number of nodes is proportional to a strict correlation among the proteins analyzed. (d) The analysis of the pathway and process enrichment derived from the Metascape analysis of the cytokines displayed in (c) showing that IL-1 β , IL-3, MCP-1, TNF- α , EGF are all related to lung fibrosis and inflammation.

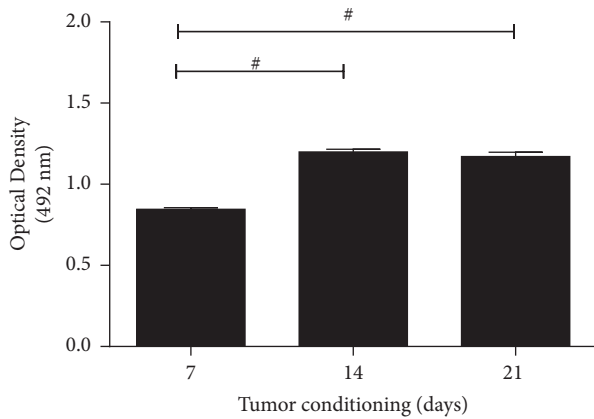


FIGURE 4: Proliferation assay of A549 after culture with supernatants of benign AMSC previously preconditioned with LAC-derived conditioned media up to 21 days and so retested on A549. The graph shows an increase in cell proliferation of A549 at 14 and 21 days compared to 7 days. Samples were normalized on basal media of AMSC. # $p < 0.001$.

regulatory role within the tissue [46]. Specifically, our data show that the difference among the secretome obtained by benign and malignant-like microenvironments of AMSC at early stages is limited to the increase of a small pool of soluble factors. Notably, among them (IL1- β , IL-3, MCP-1, TNF- α), the EGF, the most acknowledged target for lung cancer therapy [47], emerges. We also found that this set of soluble mediators is functionally interconnected and related to lung inflammation and fibrosis. The grade of fibrosis in lung cancer is a key issue and represents the modification of a permissive microenvironment induced by the continuous crosstalk between tumor and cancer-associated fibroblasts (as part of the stromal fraction), which leads to the manipulation of the extracellular matrix components and to the transition towards the epithelial-mesenchymal traits [48]. Lung fibrosis may be a prerequisite for the development of lung adenocarcinoma [49] and so is the perpetuating inflammatory condition which fosters the most suitable biological background for tumor progression [50]. Profibrotic markers (alpha-smooth muscle actin, fibrillar collagens, SMAD3) expressed in histological samples of patients with lung cancer, are correlated to low survival [51]. Other important observations derived from pulmonary idiopathic fibrosis cases and interstitial fibrosis, are considered an independent risk variable for lung adenocarcinoma [52–54]. Lung fibrosis also positively correlates with a glycolytic metabolism of the tumor in subjects with IIIA NSCLC [55].

Notably, we have provided a first biological indication of the possibility to “educate” the benign AMSC toward a malignant-like behavior. This is in line with several observations regarding the process of educating MSC [56] which has been described for bone marrow-derived MSC differentiating towards malignant phenotype, once recruited by cancer microenvironment [57]. Novel clinical applications by employing chemotherapeutic agents or enhancing CAR-T cells/-NK in cancer immunotherapy exploit the ability to educate MSC to guide the tropism of the stromal fraction [4, 58]. Our study is also coherent with additional

reports showing that tumor cells educate MSC depending on the tumor microenvironment [59], strengthening the significance of the microenvironmental control exerted by cancer.

Although we have not identified the exact molecular mechanism by which a malignant microenvironment can be also generated in the remote stromal area, we have provided a first biological correlation between the secretome (the pool of the 5 increasing soluble factors between malignant and benign microenvironments) of the stromal fraction at remote sites and changes of matched circulating and tissue miRNAs. Our data highlight how serum levels of miR-101, 126, and let-7g already reflect the same expression profile of the corresponding cancer tissue in patients with early stages of lung adenocarcinoma. The miR-486 represents an exception in our findings as its levels are downregulated and upregulated in tissue and serum, respectively. This is not surprising, considering that the decrease of miR-486 found in NSLC tissues, is inversely correlated to both lung metastasis [60] and cancer stages [61]. Plasma levels of miR-486 are reported to increase after NSLC resection [62]. Based on these findings, miR-486 is currently considered one of the most significant prognostic markers for early diagnosis in NSLC [63]. Besides, the miR-126-3p which is known as angiomiRNA and mainly produced by platelets and endothelial cells [33], is already upregulated in both cancer tissue and serum, likely suggesting a potential early involvement of a dysregulated angiogenesis towards the influence of lung adenocarcinoma at early stages. The miR-126 possesses prognostic value and its involvement in lung cancer angiogenesis has been described [64, 65]. By decreasing the proliferation through the silencing of miR-126-3p, our results suggest a specific effect on the “malignant-like” AMSC-derived media. Our explanation is that the AMSC-derived supernatants did not influence per se the level of the miR-126-3p in A549 (as it is similar to the control media up to 7 days), but rather the endogenous target/s of the miR-126-3p associated to proliferation, once cells were treated. We found that a defined pool of 5 soluble factors (EGF, IL-1b, IL-3, TNF-a, CCL2) resulted in predictive under the control of miR-126-3p. However, even the bidirectional cytokine-miRNAs relationship in inflammatory systems has been reported, where also soluble molecules are able to influence the activity of miRNAs and vice versa [66, 67]. Thus, it is plausible that the proliferative effects were mediated by those cytokines within the AMSC-derived media and miR-126 feedback loop. A main involvement in the regulation of the miR-126-associated proliferation could be the epidermal growth factor-like domain-containing gene 7 (EGFL7) a master regulator of angiogenesis and cancer pathogenesis [38, 68]. The miR-126 is encoded by EGFL7 and it may silence genes such as mTOR and PIK3R2 [69], which are all linked to cell proliferation.

Notably, the enhancement of miR-126 in A549 cultures impairs tumor cell proliferation [71]. However, these studies have been mainly performed in absence of specific treatments such as AMSC-derived conditioned media strengthening the role of miRNAs in targeting different molecular partners according to the biological stimulus applied.

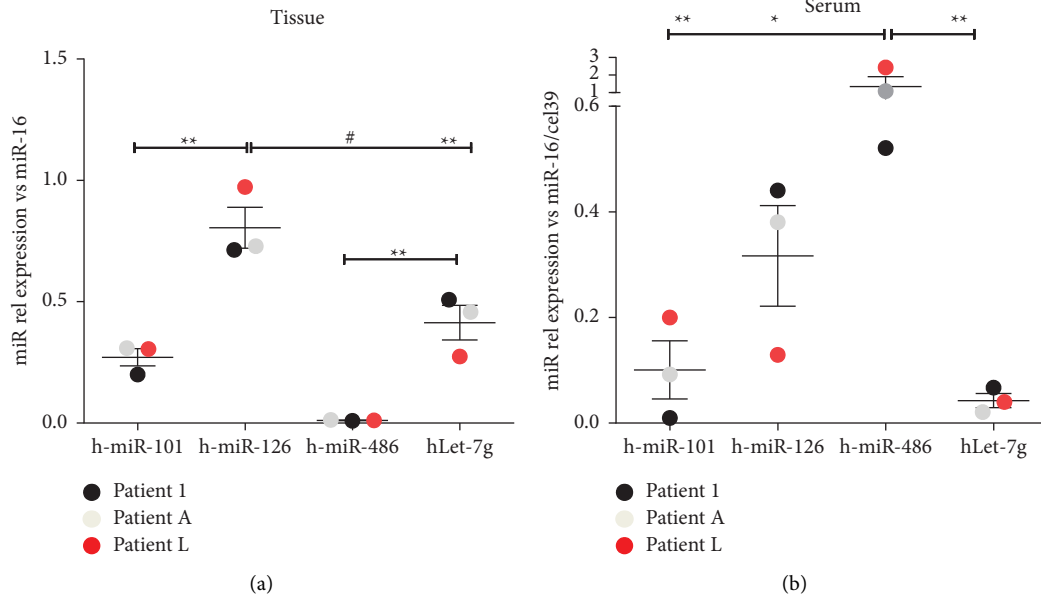


FIGURE 5: Real time PCR for miR-101, 126, 486 and let-7-g in (a) cancer tissues and the corresponding (b) sera of 3 patients with lung adenocarcinoma at early stages. Samples were normalized on miR-16 and miR-16/cell39 for tissue and sera, respectively. ** $p < 0.01$; # $p < 0.001$.

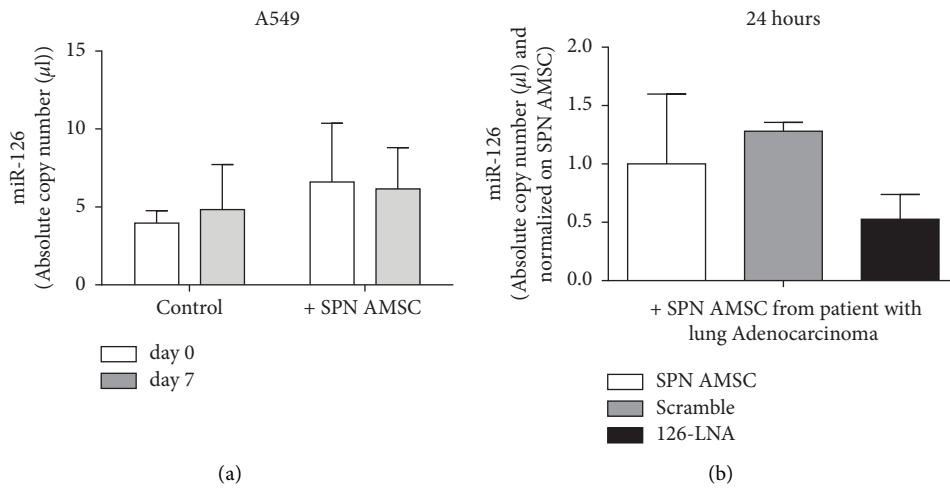


FIGURE 6: Continued.

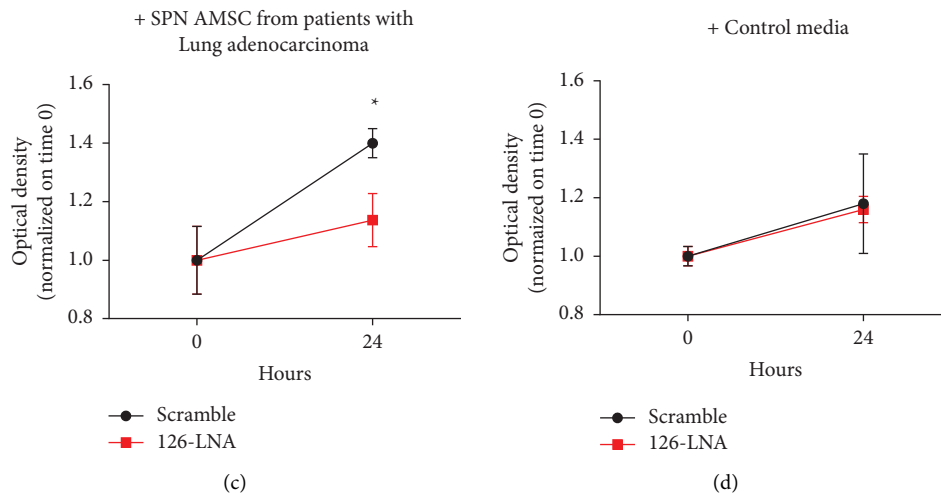


FIGURE 6: MiR-126-3p silencing in A549 cell line. (a) Absolute copy number of miR-126-3p quantified by digital droplet PCR in A549 treated with AMSC-derived supernatants from patients with lung adenocarcinoma or control basal media. (b) miR-126-3p silencing-based experiments at 24 hours in A549 conditioned with AMSC-derived supernatants from patients with lung adenocarcinoma, showing the decrease of the copy number of the endogenous miR-126-3p. Samples were normalized to the control condition. (c) MTS assay of the A549 after silencing of the endogenous miR-126-3p and treated with AMSC-derived supernatants from patients with lung adenocarcinoma, showing the significant decrease of cell proliferation after 24 hours. The effect was not reproducible in the control (d). * $p < 0.05$.

5. Conclusions

Our study has several limitations. We have not demonstrated the direct association between the soluble factors-miRNAs and systemic effect towards stromal cells at remote sites upon the influence of lung adenocarcinoma at early stages. The education of the stromal fraction cannot be also restricted to the sole secretome by cancer cells and certainly additional molecular and biological mechanisms including genomic alterations and mutations need to occur, in order to favor the progression of lung cancer. Besides, we must consider that AMSC retains the intrinsic ability to favor cell proliferation and proangiogenic properties depending on the adipose depot [20], suggesting further prudence to the use of MSC in cancer-related clinical applications.

Despite this, our study sheds further light on the complex relationship between cancer and stromal compartment mediated by the microenvironment to communicate with niches at remote sites.

Data Availability

Main data generated or analyzed during this study are included in this article, and detailed data are available from the corresponding authors upon reasonable request.

Ethical Approval

The methodology described in this study has been conducted in compliance with the tenets of the Declaration of Helsinki for experiments involving human tissues. This study was approved by the Ethical Committee of S. Andrea Hospital, Rome (Prot. CE N. 5195/2013). Medical records of each patient were collected in a clinical database. All data were deidentified and analyzed anonymously.

Conflicts of Interest

The authors declare that they have no conflict of interest.

Authors' Contributions

EDF wrote the manuscript and conceived the study; AB cultured the cells; XD performed the informatic analysis; VP performed the cytofluorimetry; CZ and EF performed the miRNA interfering experiments; EDM performed the digital droplet PCR experiments; NG evaluated histology; PR performed statistics; CM, ER, and MI performed the surgery; AC conceived the study and revised the manuscript.

Acknowledgments

The authors would like to thank the Department of Medical-Surgical Science and Biotechnologies based in Latina for its continuous support. This work was supported by the Sapienza University of Rome Prot. N. C26A13SC2R and Prot, N. AR22218167F02218 granted to Elena De Falco and Antonella Bordin, respectively.

Supplementary Materials

Clinical characteristics of adipose tissue-derived MSC samples and the apoptotic rate of the cell cultures treated with MSC-derived supernatants are reported in the supplementary table 1a-b and Figure 1a-b, respectively. (*Supplementary Materials*)

References

- [1] C. Siciliano, I. Chimenti, A. Bordin et al., "The potential of GMP-compliant platelet lysate to induce a permissive state for cardiovascular transdifferentiation in human mediastinal adipose tissue-derived mesenchymal stem cells," *BioMed Research International*, vol. 2015, pp. 1-10, 2015.

- [2] C. Siciliano, M. Ibrahim, G. Scafetta et al., "Optimization of the isolation and expansion method of human mediastinal-adipose tissue derived mesenchymal stem cells with virally inactivated GMP-grade platelet lysate," *Cytotechnology*, vol. 67, no. 1, pp. 165–174, 2015.
- [3] T. Lan, M. Luo, and X. Wei, "Mesenchymal stem/stromal cells in cancer therapy," *Journal of Hematology & Oncology*, vol. 14, no. 1, p. 195, 2021.
- [4] L. Y. Chan, S. A. Dass, G. J. Tye, S. A. M. Imran, W. S. Wan Kamarul Zaman, and F. Nordin, "CAR-T cells/-NK cells in cancer immunotherapy and the potential of MSC to enhance its efficacy: a review," *Biomedicines*, vol. 10, no. 4, p. 804, 2022.
- [5] Z. Wang, H. Chen, P. Wang et al., "Site-specific integration of TRAIL in iPSC-derived mesenchymal stem cells for targeted cancer therapy," *Stem Cells Translational Medicine*, vol. 11, no. 3, pp. 297–309, 2022.
- [6] C. Choe, Y. S. Shin, S. H. Kim et al., "Tumor-stromal interactions with direct cell contacts enhance motility of non-small cell lung cancer cells through the hedgehog signaling pathway," *Anticancer Research*, vol. 33, no. 9, pp. 3715–3723, 2013.
- [7] S. M. Ridge, F. J. Sullivan, and S. A. Glynn, "Mesenchymal stem cells: key players in cancer progression," *Molecular Cancer*, vol. 16, no. 1, p. 31, 2017.
- [8] R. A. Salah, M. A. Nasr, A. M. El-Derby et al., "Hepatocellular carcinoma cell line-microenvironment induced cancer-associated phenotype, genotype and functionality in mesenchymal stem cells," *Life Sciences*, vol. 288, Article ID 120168, 2022.
- [9] N. Erin, J. Grahovac, A. Brozovic, and T. Efferth, "Tumor microenvironment and epithelial mesenchymal transition as targets to overcome tumor multidrug resistance," *Drug Resistance Updates*, vol. 53, Article ID 100715, 2020.
- [10] R. Hass, "Role of MSC in the tumor microenvironment," *Cancers*, vol. 12, no. 8, p. 2107, 2020.
- [11] A. Mohammadalipour, S. P. Dumbali, and P. L. Wenzel, "Mitochondrial transfer and regulators of mesenchymal stromal cell function and therapeutic efficacy," *Frontiers in Cell and Developmental Biology*, vol. 8, Article ID 603292, 2020.
- [12] M. Timaner, K. K. Tsai, and Y. Shaked, "The multifaceted role of mesenchymal stem cells in cancer," *Seminars in Cancer Biology*, vol. 60, pp. 225–237, 2020.
- [13] R. Liu, S. Wei, J. Chen, and S. Xu, "Mesenchymal stem cells in lung cancer tumor microenvironment: their biological properties, influence on tumor growth and therapeutic implications," *Cancer Letters*, vol. 353, no. 2, pp. 145–152, 2014.
- [14] O. L. Chinot, W. Wick, W. Mason et al., "Bevacizumab plus radiotherapy-temozolomide for newly diagnosed glioblastoma," *New England Journal of Medicine*, vol. 370, no. 8, pp. 709–722, 2014.
- [15] F. Vakhshiteh, F. Atyabi, and S. N. Ostad, "Mesenchymal stem cell exosomes: a two-edged sword in cancer therapy," *International Journal of Nanomedicine*, vol. 14, pp. 2847–2859, 2019.
- [16] E. Spaeth, A. Klopp, J. Dembinski, M. Andreeff, and F. Marini, "Inflammation and tumor microenvironments: defining the migratory itinerary of mesenchymal stem cells," *Gene Therapy*, vol. 15, no. 10, pp. 730–738, 2008.
- [17] M. Yu, A. Bardia, B. S. Wittner et al., "Circulating breast tumor cells exhibit dynamic changes in epithelial and mesenchymal composition," *Science*, vol. 339, no. 6119, pp. 580–584, 2013.
- [18] T. Tayoun, V. Faugeroux, M. Oulhen, A. Aberlenc, P. Pawlikowska, and F. Farace, "CTC-derived models: a window into the seeding capacity of circulating tumor cells (CTCs)," *Cells*, vol. 8, no. 10, p. 1145, 2019.
- [19] P. Collas, "Programming differentiation potential in mesenchymal stem cells," *Epigenetics*, vol. 5, no. 6, pp. 476–482, 2010.
- [20] C. Siciliano, A. Bordin, M. Ibrahim et al., "The adipose tissue of origin influences the biological potential of human adipose stromal cells isolated from mediastinal and subcutaneous fat depots," *Stem Cell Research*, vol. 17, no. 2, pp. 342–351, 2016.
- [21] Z. Gao, L. Zhang, J. Hu, and Y. Sun, "Mesenchymal stem cells: a potential targeted-delivery vehicle for anti-cancer drug, loaded nanoparticles," *Nanomedicine: Nanotechnology, Biology and Medicine*, vol. 9, no. 2, pp. 174–184, 2013.
- [22] Z. Y. Bian, G. Li, Y. K. Gan, Y. Q. Hao, W. T. Xu, and T. T. Tang, "Increased number of mesenchymal stem cell-like cells in peripheral blood of patients with bone sarcomas," *Archives of Medical Research*, vol. 40, no. 3, pp. 163–168, 2009.
- [23] S. Gottschling, M. Granzow, R. Kuner et al., "Mesenchymal stem cells in non-small cell lung cancer—different from others? Insights from comparative molecular and functional analyses," *Lung Cancer*, vol. 80, no. 1, pp. 19–29, 2013.
- [24] V. B. Fernandez Vallone, E. L. Hofer, H. Choi et al., "Behaviour of mesenchymal stem cells from bone marrow of untreated advanced breast and lung cancer patients without bone osteolytic metastasis," *Clinical & Experimental Metastasis*, vol. 30, no. 3, pp. 317–332, 2013.
- [25] J. Wels, R. N. Kaplan, S. Rafii, and D. Lyden, "Migratory neighbors and distant invaders: tumor-associated niche cells," *Genes Development*, vol. 22, no. 5, pp. 559–574, 2008.
- [26] J. Majidpoor and K. Mortezaee, "Steps in metastasis: an updated review," *Medical Oncology*, vol. 38, no. 1, p. 3, 2021.
- [27] E. De Falco, A. Bordin, C. Menna et al., "Remote adipose tissue-derived stromal cells of patients with lung adenocarcinoma generate a similar malignant microenvironment of the lung stromal counterpart," *bioRxiv*, Article ID 499306, 2022.
- [28] R. Businaro, E. Scaccia, A. Bordin et al., "Platelet lysate-derived neuropeptide γ influences migration and angiogenesis of human adipose tissue-derived stromal cells," *Scientific Reports*, vol. 8, no. 1, Article ID 14365, 2018.
- [29] C. Menna, E. De Falco, L. Pacini et al., "Axitinib affects cell viability and migration of a primary foetal lung adenocarcinoma culture," *Cancer Investigation*, vol. 32, no. 1, pp. 13–21, 2014.
- [30] D. Bastianelli, C. Siciliano, R. Puca et al., "Influence of Egr-1 in cardiac tissue-derived mesenchymal stem cells in response to glucose variations," *BioMed Research International*, vol. 2014, pp. 1–11, 2014.
- [31] E. De Falco, G. Scafetta, C. Siciliano et al., "GMP-grade platelet lysate enhances proliferation and migration of tenon fibroblasts," *Frontiers in Bioscience*, vol. 8, no. 1, pp. 753–799, 2016.
- [32] S. Gao, J. Wang, Q. Zhang et al., "Cytokine antibody array-based analysis of IL-37 treatment effects in asthma," *Aging (Albany NY)*, vol. 13, no. 17, pp. 21729–21742, 2021.
- [33] A. Bordin, M. Chirivi, F. Pagano et al., "Human platelet lysate-derived extracellular vesicles enhance angiogenesis through miR-126," *Cell Proliferation*, vol. 55, no. 11, Article ID e13312, 2022.
- [34] Y. Zhou, B. Zhou, L. Pache et al., "Metascape provides a biologist-oriented resource for the analysis of systems-level

- datasets,” *Nature Communications*, vol. 10, no. 1, p. 1523, 2019.
- [35] E. Miotto, E. Saccenti, L. Lupini, E. Callegari, M. Negrini, and M. Ferracin, “Quantification of circulating miRNAs by droplet digital PCR: comparison of EvaGreen- and TaqMan-based chemistries,” *Cancer Epidemiology, Biomarkers & Prevention*, vol. 23, no. 12, pp. 2638–2642, 2014.
- [36] J. Lawson, C. Dickman, S. MacLellan et al., “Selective secretion of microRNAs from lung cancer cells via extracellular vesicles promotes CAMK1D-mediated tube formation in endothelial cells,” *Oncotarget*, vol. 8, no. 48, pp. 83913–83924, 2017.
- [37] J. Yang, H. Lan, X. Huang, B. Liu, and Y. Tong, “MicroRNA-126 inhibits tumor cell growth and its expression level correlates with poor survival in non-small cell lung cancer patients,” *PLoS One*, vol. 7, no. 8, Article ID e42978, 2012.
- [38] Q. Chen, S. Chen, J. Zhao, Y. Zhou, and L. Xu, “MicroRNA-126: a new and promising player in lung cancer (Review),” *Oncology Letters*, vol. 21, no. 1, p. 1, 2020.
- [39] A. Tirpe, D. Gulei, G. R. Tirpe et al., “Beyond conventional: the new horizon of anti-angiogenic microRNAs in non-small cell lung cancer therapy,” *International Journal of Molecular Sciences*, vol. 21, no. 21, p. 8002, 2020.
- [40] K. J. Hiam-Galvez, B. M. Allen, and M. H. Spitzer, “Systemic immunity in cancer,” *Nature Reviews Cancer*, vol. 21, no. 6, pp. 345–359, 2021.
- [41] L. M. Coussens and Z. Werb, “Inflammation and cancer,” *Nature*, vol. 420, no. 6917, pp. 860–867, 2002.
- [42] K. Pietras and A. Ostman, “Hallmarks of cancer: interactions with the tumor stroma,” *Experimental Cell Research*, vol. 316, no. 8, pp. 1324–1331, 2010.
- [43] A. J. Redig and S. S. McAllister, “Breast cancer as a systemic disease: a view of metastasis,” *Journal of Internal Medicine*, vol. 274, no. 2, pp. 113–126, 2013.
- [44] Y. Kang and K. Pantel, “Tumor cell dissemination: emerging biological insights from animal models and cancer patients,” *Cancer Cell*, vol. 23, no. 5, pp. 573–581, 2013.
- [45] D. Hanahan, “Hallmarks of cancer: new dimensions,” *Cancer Discovery*, vol. 12, no. 1, pp. 31–46, 2022.
- [46] D. C. Hinshaw and L. A. Shevde, “The tumor microenvironment innately modulates cancer progression,” *Cancer Research*, vol. 79, no. 18, pp. 4557–4566, 2019.
- [47] M. D. Siegelin and A. C. Borczuk, “Epidermal growth factor receptor mutations in lung adenocarcinoma,” *Laboratory Investigation*, vol. 94, no. 2, pp. 129–137, 2014.
- [48] J. C. Becker, M. H. Andersen, D. Schrama, and P. Thor Straten, “Immune-suppressive properties of the tumor microenvironment,” *Cancer Immunology Immunotherapy*, vol. 62, no. 7, pp. 1137–1148, 2013.
- [49] B. Mehic, L. Duranovic Rayan, N. Bilalovic, D. Dohranovic Tafro, and I. Pilav, “Lung adenocarcinoma mimicking pulmonary fibrosis—a case report,” *BMC Cancer*, vol. 16, no. 1, p. 729, 2016.
- [50] S. Lantuejoul, T. V. Colby, G. R. Ferretti, P. Y. Bricchon, C. Brambilla, and E. Brambilla, “Adenocarcinoma of the lung mimicking inflammatory lung disease with honeycombing,” *European Respiratory Journal*, vol. 24, no. 3, pp. 502–505, 2004.
- [51] R. Ikemori, M. Gabasa, P. Duch et al., “Epigenetic SMAD3 repression in tumor-associated fibroblasts impairs fibrosis and response to the antifibrotic drug nintedanib in lung squamous cell carcinoma,” *Cancer Research*, vol. 80, no. 2, pp. 276–290, 2020.
- [52] Y. Yoneshima, E. Iwama, S. Matsumoto et al., “Paired analysis of tumor mutation burden for lung adenocarcinoma and associated idiopathic pulmonary fibrosis,” *Scientific Reports*, vol. 11, no. 1, Article ID 12732, 2021.
- [53] J. Li, M. Yang, P. Li, Z. Su, P. Gao, and J. Zhang, “Idiopathic pulmonary fibrosis will increase the risk of lung cancer,” *Chinese Medical Journal*, vol. 127, no. 17, pp. 3142–3149, 2014.
- [54] E. Barczi, T. Nagy, L. Starobinski et al., “Impact of interstitial lung disease and simultaneous lung cancer on therapeutic possibilities and survival,” *Thoracic Cancer*, vol. 11, no. 7, pp. 1911–1917, 2020.
- [55] A. Cruz-Bermudez, R. Laza-Briviesca, R. J. Vicente-Blanco et al., “Cancer-associated fibroblasts modify lung cancer metabolism involving ROS and TGF-beta signaling,” *Free Radical Biology and Medicine*, vol. 130, pp. 163–173, 2019.
- [56] B. S. Hill, A. Pelagalli, N. Passaro, and A. Zannetti, “Tumor-educated mesenchymal stem cells promote pro-metastatic phenotype,” *Oncotarget*, vol. 8, no. 42, pp. 73296–73311, 2017.
- [57] B. Sai, Y. Dai, S. Fan et al., “Cancer-educated mesenchymal stem cells promote the survival of cancer cells at primary and distant metastatic sites via the expansion of bone marrow-derived-PMN-MDSCs,” *Cell Death & Disease*, vol. 10, no. 12, p. 941, 2019.
- [58] M. Timaner, N. Letko-Khait, R. Kotsofruk et al., “Therapy-Educated mesenchymal stem cells enrich for tumor-initiating cells,” *Cancer Research*, vol. 78, no. 5, pp. 1253–1265, 2018.
- [59] A. Le Naour, M. Prat, B. Thibault et al., “Tumor cells educate mesenchymal stromal cells to release chemoprotective and immunomodulatory factors,” *Journal of Molecular Cell Biology*, vol. 12, no. 3, pp. 202–215, 2020.
- [60] M. Jiang, X. Li, X. Quan et al., “MiR-486 as an effective biomarker in cancer diagnosis and prognosis: a systematic review and meta-analysis,” *Oncotarget*, vol. 9, no. 17, pp. 13948–13958, 2018.
- [61] M. A. Mohamed, E. I. Mohamed, S. A. A. El-Kaream, M. I. Badawi, and S. H. Darwish, “Underexpression of miR-486-5p but not overexpression of miR-155 is associated with lung cancer stages,” *MicroRNA*, vol. 7, no. 2, pp. 120–127, 2018.
- [62] M. Sromek, M. Glogowski, M. Chechlinska et al., “Changes in plasma miR-9, miR-16, miR-205 and miR-486 levels after non-small cell lung cancer resection,” *Cellular Oncology*, vol. 40, no. 5, pp. 529–536, 2017.
- [63] W. Li, Y. Wang, Q. Zhang et al., “Correction: MicroRNA-486 as a biomarker for early diagnosis and recurrence of non-small cell lung cancer,” *PLoS One*, vol. 11, no. 1, Article ID e0148589, 2016.
- [64] L. Sun, H. Zhou, Y. Yang et al., “Meta-analysis of diagnostic and prognostic value of miR-126 in non-small cell lung cancer,” *Bioscience Reports*, vol. 40, no. 5, Article ID BSR20200349, 2020.
- [65] Y. Wang, J. Shi, Y. Wu et al., “Use of Luminex xMAP bead-based suspension array for detecting microRNA in NSCLC tissues and its clinical application,” *Tumori*, vol. 98, no. 6, pp. 792–799, 2012.
- [66] T. Amado, N. Schmolka, H. Metwally, B. Silva-Santos, and A. Q. Gomes, “Cross-regulation between cytokine and microRNA pathways in T cells,” *European Journal of Immunology*, vol. 45, no. 6, pp. 1584–1595, 2015.
- [67] A. Jafarzadeh, M. Nemati, N. Aminizadeh et al., “Bidirectional cytokine-microRNA control: a novel immunoregulatory framework in leishmaniasis,” *PLoS Pathogens*, vol. 18, no. 8, Article ID e1010696, 2022.
- [68] G. Hong, V. Kuek, J. Shi et al., “EGFL7: master regulator of cancer pathogenesis, angiogenesis and an emerging mediator

- of bone homeostasis,” *Journal of Cellular Physiology*, vol. 233, no. 11, pp. 8526–8537, 2018.
- [69] L. Song, D. Li, Y. Gu et al., “MicroRNA-126 targeting PIK3R2 inhibits NSCLC A549 cell proliferation, migration, and invasion by regulation of PTEN/PI3K/AKT pathway,” *Clinical Lung Cancer*, vol. 17, no. 5, pp. e65–e75, 2016.
- [70] X. Zhu, H. Li, L. Long et al., “miR-126 enhances the sensitivity of non-small cell lung cancer cells to anticancer agents by targeting vascular endothelial growth factor A,” *Acta Biochimica et Biophysica Sinica*, vol. 44, no. 6, pp. 519–526, 2012.